crystals

MDPI

Communication

Feasibility Study of Selective Laser Melting for Metal Matrix Diamond Tools

Xiaohong Fang [1], Zhan Yang [2], Songcheng Tan [1,*] and Longchen Duan [1]

[1] Faculty of Engineering, China University of Geosciences, Wuhan 430074; China; duyaoff@163.com (X.F.); duanlongchen@163.com (L.D.)

[2] School of Mechanical Engineering and Electronic Information, China University of Geosciences, Wuhan 430074, China; fifasheep@126.com

* Correspondence: wstansongcheng@cug.edu.cn

Received: 17 June 2020; Accepted: 7 July 2020; Published: 10 July 2020

check for updates

Abstract: Metal matrix diamond composite samples were fabricated by selective laser melting (SLM) at different forming parameters to investigate the feasibility and new challenges when SLM is applied to diamond tools manufacturing. The surface topographies, Rockwell hardness, compactness, microstructure, and diamond thermal damage of the samples were investigated in this study. The fabricated samples had high porosity and relatively low Rockwell hardness and compactness, and some ridge-shaped bulges and textures were observed at the edges and surfaces. Microstructure analyses showed that diamond particles were homogeneously distributed and metallurgically bonded within the metal matrix. The thermal damage pits on the diamond crystals along the scanning direction were the dominant damage type for SLM, which was completely different from conventional vacuum brazing and hot-pressing sintering. Although some challenges need to be further studied, our results demonstrate that SLM has great potential to propel the development of metal matrix diamond tools.

Keywords: metal matrix composites; particle reinforcement; 3-D printing, microstructure; thermal damage

1. Introduction

Diamond tools refer to products that contain diamond in their texture as a key element [1–3]. Diamond tools can be generally divided into resin, ceramic, and metal types based on their matrix material [4]. Among these, the metal matrix diamond composite (MMDC) has the highest strength and is widely used in the manufacture of various types of diamond cutting and drilling tools. In order to improve the service performance of metal matrix diamond tools, many studies were conducted mainly in manufacturing process [5–7], metal matrix formula systems [8–11], and structure design aspects [12–14]. However, a theoretically optimized tool structure faces some challenges when it comes to mold design, assembly, and the manufacturing process. Therefore, because of their poor service stability, it is difficult to mass-produce and popularize the specially designed diamond tools. Currently, a 3-D printing technology called selective laser melting (SLM) has been widely applied in the aerospace, biomedical, automobile, mold, and jewelry fields [15–19]. SLM technology can transfer complex 3-D manufacturing into simple 2-D manufacturing and has obvious advantages for tools with complex structures and thus can provide a potential solution to the above-mentioned problems. The aim of this study is to investigate the feasibility of using SLM and to identify the main challenges in manufacturing metal matrix diamond tools with special structural characteristics.

2. Experimental Details

The commercially available FJT-A5 pre-alloyed powder (Ni10Co10Cu40Sn9Fe31, Hunan Fulong New Materials Co. LTD, Changsha, China) and SMD40 diamond particles (Changsha Jiesheng Superhard Materials Co. LTD, Changsha, China) were used in this study. The average size of metal powder was 48 μm, the average sizes of diamond particles were between 180 and 212 μm, and diamond volume concentration was 20 vol.%. The metal powder and diamond particles were mechanically mixed for 4 h before being fed to the HK M125 SLM machine (Huake 3D Technology Co. Ltd, Wuhan, China). The working chamber was filled with argon gas to avoid oxidation.

The laser beams produced by the HK M125 SLM machine are continuous waves with an emission wavelength of 1070 ± 10 nm and an emission bandwidth of less than 6 nm. The recommended layer thickness is 0.02–0.1 mm. Nevertheless, based on the metal composition and the metal powder and diamond particles sizes, the selected SLM parameters were as follows: laser power of 180 to 200 W, scanning speed of 700 to 900 mm s^{-1}, hatch spacing of 0.07 mm, and layer thickness of 0.3 mm. The dimensions of the MMDC samples were 20 mm × 20 mm × 6 mm. Detailed scanning speed and laser power for each sample are shown in Table 1.

Table 1. Detailed scanning parameters for the selective laser melting (SLM) manufactured samples.

Sample Number	Laser Power (W)	Scanning Speed ($mm \cdot s^{-1}$)	Volume Energy Density ($J \cdot mm^{-3}$)
1	180	700	12.24
2	200	700	13.61
3	160	800	9.52
4	180	800	10.71
5	200	800	11.90
6	160	900	8.47
7	180	900	9.52
8	200	900	10.58

A laser scanning confocal microscope (VK-X100K, Keyence, Osaka, Japan) was used to study the surface topography of the samples. The hardness of the samples was tested by a Rockwell hardness Tester (HR150, Yexian Testing Machine, Yexian, China), and samples' microstructure was studied using a scanning electron microscope (G2 Pro, Phenom, Eindhoven, Netherlands).

3. Results and Discussion

3.1. Surface Topographies and Hardness

As shown in Figure 1a, to a certain degree, eight samples show similar macroscopic topography. Local micro-morphologies indicated that there were no specific differences between the eight samples. Consequently, Figure 1b–d shows the macroscopic, 2-D and 3-D local micro-morphologies of sample 2 as an example. As shown in Fig 1b, ridge-shaped bulges and textures were observed at the edges and surfaces of the sample in macroscopic scale. As the samples were formed by layers of melted and superimposed metal powders, these bulges and textures are likely to have affected the dimensional accuracy of the samples. Figure 1c,d indicates height differences of up to 400 μm or higher on the sample surface. The height difference is more remarkable as the thickness of the sample increases.

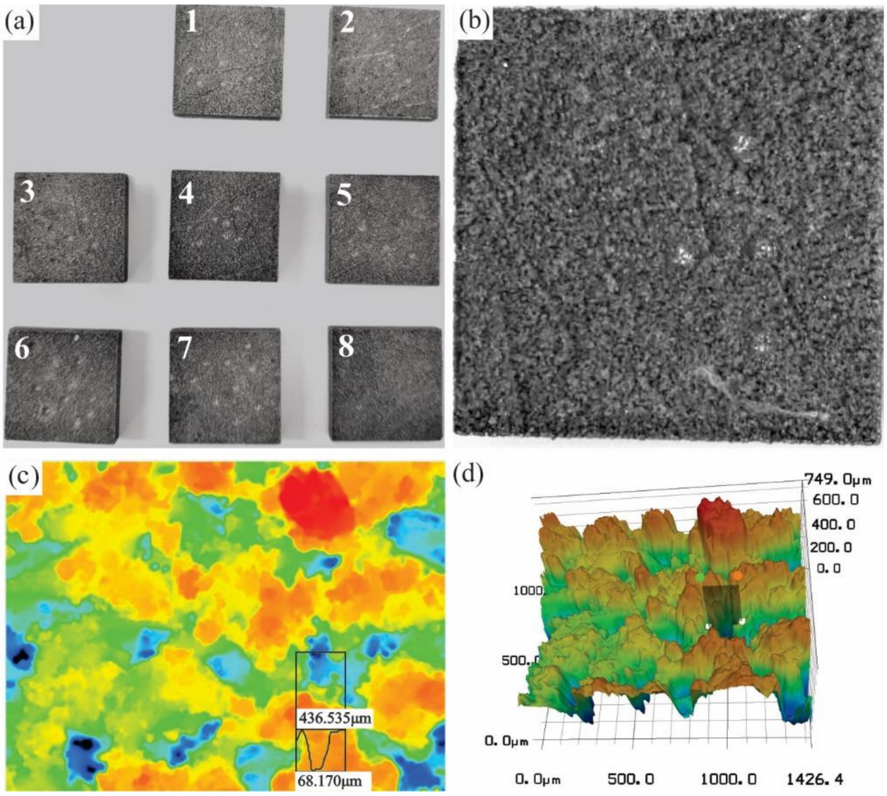

Figure 1. Topographies of sample 2 manufactured by SLM. (**a**) Samples manufactured by SLM; (**b**) macroscopic features show the bulges and textures caused by hatch spacing; (**c**) and (**d**) show the 2-D and 3-D local micro-morphologies of sample surface.

According to Table 1 and Figure 2, scanning parameters have significant effects on the hardness and compactness of the samples. Figure 2a indicates that sample hardness decreases monotonically with increasing scanning speed, whereas it increases with an increase in the laser power. Looked at from another perspective in Figure 2b, however, these results show that sample hardness increases monotonically with the volume energy density overall, which is actually due to the modest improvement of sample compactness. Within the tested scanning parameters, the attached sample compactness ranges from 55.95% to 70.23%, while the sample hardness ranges from 22 HRB to 72 HRB.

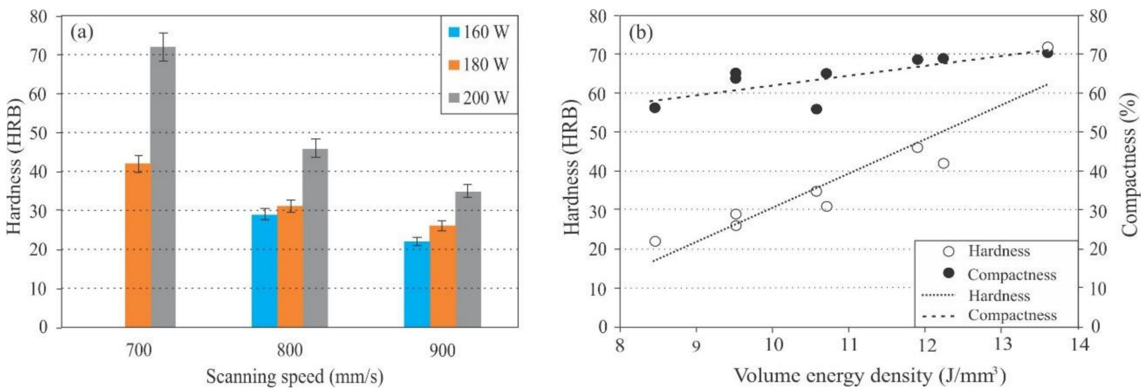

Figure 2. Effects of scanning parameters on the Rockwell hardness and compactness of SLM manufactured samples. (**a**) Scanning speed and laser power on the sample hardness; (**b**) volume energy density on the sample hardness and compactness.

The preferred metal powder sizes for SLM are 25 to 45 μm with a high spherical degree [20,21]. The layer thickness should also not be more than 0.1 mm [22]. However, in this study, the diamond particle sizes (180–212 μm) were much larger than the metal powder size (48 μm), which resulted in higher than normal layer thickness. A thicker layer allowed for bigger diamond sizes, while higher laser power, lower scanning speed, and smaller hatch spacing ensured a better diamond composite, which met the design and manufacturing requirements. As shown in Figure 2, the highest hardness reached was 72 HRB at a scanning speed of 700 mm s^{-1} and laser power of 200 W. Although this value may not be high enough for impregnated diamond bits, it is sufficient for diamond circular saws already.

Higher surface roughness is usually a disadvantage for the performance of precision machining tools, but it could be an advantage for cutting tools, such as impregnated diamond bits and saw blades. The rough surface in Figure 1b is helpful in increasing the unit cutting pressure of the tool, thus improving the cutting efficiencies of the drill bits and saw blades. The textured surface also has a positive effect on reducing the friction coefficient and drag force between the cutting tools and targeted objects [23].

3.2. Microstructure

Figure 3a shows that the diamond particles, marked by circles, are distributed relatively homogeneously within a local region of MMDC. The difficulty of fully melting the pre-alloyed metal powder at the selected laser power and scanning speeds when the layer was too thick is also shown in this figure. Due to this issue, a large number of micro-pores were generated within the MMDC samples, diminishing their compactness and hardness.

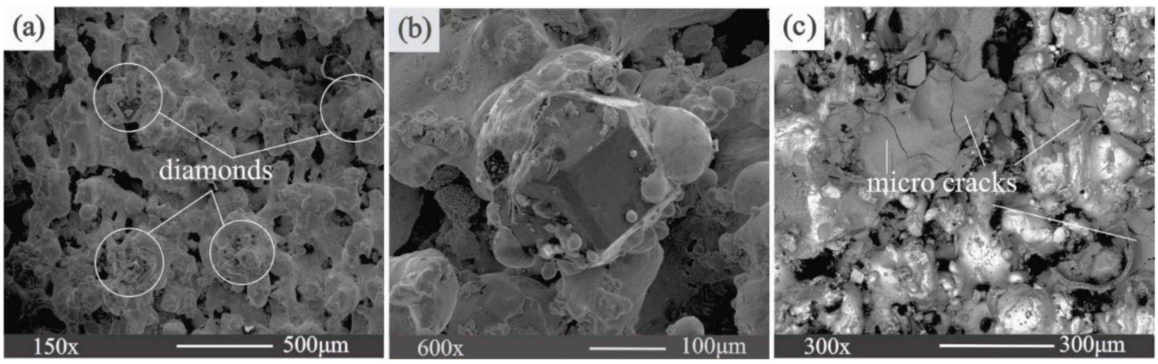

Figure 3. SEM images of metal matrix diamond composite (MMDC) samples manufactured by SLM, showing the occurrence of diamond particles and microstructure features of metal matrix: (**a**) Diamond distribution and high porosity of MMDC; (**b**) an undamaged diamond particle and its wrapped morphology; (**c**) micro-cracks on a metal matrix.

Figure 3b shows the occurrence of a single diamond particle in the MMDC, indicating that diamond particles could still maintain good crystal shapes and complete crystal surfaces if they were not scanned by laser beams. It is also shown in Figure 3b that the melted liquid metal, due to high laser power, might cause the formation of a metallurgical bonding between the diamond surfaces and the metal matrix as there is no obvious gap between these two materials.

On the one hand, the metallurgical bonding can enhance the strength of the metal matrix in holding diamond particles [24–26], which improves the service performance of diamond tools. On the other hand, typically for impregnated diamond bit drilling process, high porosity might result in lower mechanical strength and cause abnormal fractures during the service process, which adversely affect the service performance of diamond tools. Therefore, improving the compactness of MMDC in thick layers needs to be further investigated in the future.

Figure 3c shows some apparent micro-cracks on the surface of the MMDC sample. Micro-cracks caused by rapid melting and condensation of metal materials are one of the most common defects in the SLM forming industry [15,27]. The high temperature gradient leads to excessive internal residual stress within the composite, which induces micro-cracks [28]. Therefore, quantitative measurement of the residual stress and efficient methods to reduce micro-cracks need further investigation.

3.3. Thermal Damage to Diamond Particles

Figure 4a shows a diamond particle located exactly on the laser scanning path that resulted in two rows of thermal damage pits along the laser scanning direction on that surface. The damage pits were caused by high laser power, and the depth and numbers of the pits were closely related to laser power and scanning speed. However, Figure 4a shows that the damage was limited, because the crystal shape and other diamond surfaces are still intact. Figure 4b shows that the thermal damage caused by vacuum brazing is mainly manifested as surface graphitization [29]. The thickness of the graphite layer is closely related to the brazing material compositions and the brazing process. Additionally, as a result of the high brazing temperature, micro-cracks might be induced within the metal matrix. Figure 4c shows the extreme graphitization of a diamond particle caused by hot-pressing sintering [30]. The diamond crystal surface and crystal shape both deteriorated due to the scaly chipping on the diamond particle surfaces. There is no metallurgical bonding between the diamond particles and metal matrix. Therefore, the diamond particle is just mechanically embedded in the metal matrix, which leads to an obvious micro-gap at the interface of the diamond particle surface and metal matrix.

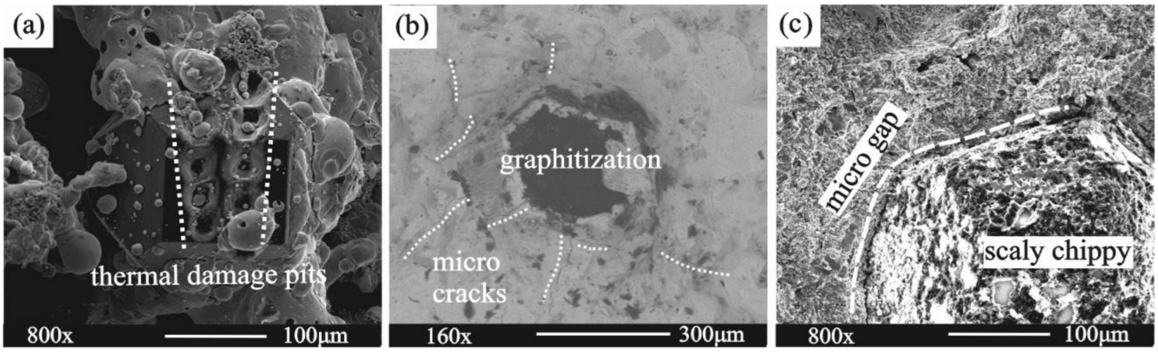

Figure 4. SEM images showing the effects of manufacturing methods on diamond thermal damage: (**a**) SLM; (**b**) vacuum brazing; (**c**) hot-pressing sintering.

These comparisons demonstrate that the thermal damage caused by the three manufacturing methods is completely different. In spite of the thermal damage pits caused by laser beam, SLM may generate metallurgical bonding between the diamond surface and metal matrix. At the same time, graphitization to the diamond surface could be diminished because of the rapid melting and solidification processes. Therefore, a key challenge in adapting SLM in manufacturing metal matrix diamond tools is the development of an advanced technology to avoid diamond thermal damage by high power laser beams. As an example, an online recognition system could be designed for recognizing the diamond particles and metal powder in real-time during the laser scanning process, to ensure that the laser beam skips the diamond particles. Such advancements can increase the potential benefits of SLM and enhance the service performances of the metal matrix diamond tools.

4. Conclusions

(1) SLM has great prospects for application in the design and manufacturing of metal matrix diamond tools, although detailed fabricating technologies need to be further studied.

(2) In this study, hardness of the MMDC samples manufactured by SLM was limited due to large layer thickness, with the highest value of 72 HRB.

(3) Diamond particles in the SLM-formed composites are held more strongly by the metal matrix than the ones formed by vacuum brazing and hot-pressing sintering and suffer lower thermal damage.
(4) Defects such as high porosity, micro-cracks, and thermal damage pits are the main challenges that need to be overcome for future applications of the technology.

Author Contributions: Writing—original draft preparation: X.F. and S.T.; measurement and data analysis: X.F., S.T., and Z.Y.; methodology: Z.Y.; supervision: L.D. All authors have read and agreed to the published version of the manuscript.

Funding: This research was funded by National Natural Science Foundation of China, grant numbers 41602373.

Acknowledgments: The authors want to acknowledge Huake 3D Technology Co. Ltd. for technical support, Kaihua Yang and Yan Zhou for scientific discussion.

Conflicts of Interest: The authors declare no conflict of interest.

References

1. Igharo, M.; Russell, J. Experimental study development of diamond impregnated cutting tools. *Surf. Eng.* **1994**, *10*, 52–55. [CrossRef]
2. Konstanty, J. Production parameters and materials selection of powder metallurgy diamond tools. *Powder Metall.* **2006**, *49*, 299–306. [CrossRef]
3. Palyanov, Y.N. The many facets of diamond crystals. *Crystals* **2018**, *8*, 72. [CrossRef]
4. Duan, L.; Pan, B.; Fang, X. *Design and Manufacture of Diamond Tools*; China University of Geosciences Press: Wuhan, China, 2013.
5. Zhang, Y.; Pan, B. The effect of valine on the process of nickel electrocrystallization on glassy carbon electrode. *J. Electroanal. Chem.* **2017**, *796*, 43–48. [CrossRef]
6. Li, M.; Sun, Y.; Meng, Q.; Wu, H.; Gao, K.; Liu, B. Fabrication of Fe-Based Diamond Composites by Pressureless Infiltration. *Materials* **2016**, *9*, 1006. [CrossRef] [PubMed]
7. Yang, Z.; Tan, S.; Yang, K. Experimental research on metal-based diamond composites by 3D printing. *Diam. Abras. Eng* **2018**, *1*, 50–54.
8. Zaitsev, A.A.; Sidorenko, D.A.; Levashov, E.A.; Kurbatkina, V.V.; Rupasov, S.I.; Andreev, V.A.; Sevast'yanov, P.V. Development and application of the Cu-Ni-Fe-Sn-based dispersion-hardened bond for cutting tools of superhard materials. *J. Superhard Mater.* **2012**, *34*, 270–280. [CrossRef]
9. Pan, B.; Yang, Y.; Zhang, Y.; Zhang, Q. Effects of saccharin and tetramethylammonium bromide on the microstructure and microhardness of thick cobalt electrodeposits. *Surf. Coat. Tech.* **2017**, *329*, 49–54. [CrossRef]
10. Chu, Z.Q.; Guo, X.Y.; Liu, D.H.; Tan, Y.X.; Li, D.; Tian, Q.H. Application of pre-alloyed powders for diamond tools by ultrahigh pressure water atomization. *Trans. Nonferrous Met. Soc. China* **2016**, *26*, 2665–2671. [CrossRef]
11. Oliveira, F.A.C.; Anjinho, C.A.; Coelho, A.; Amaral, P.M.; Coelho, M. PM materials selection: The key for improved performance of diamond tools. *Metal Powder Rep.* **2017**, *72*, 339–344. [CrossRef]
12. Wang, J.; Zhang, S. A new diamond bit for extra-hard, compact and nonabrasive rock formation. *J. Cent. South Univ.* **2015**, *22*, 1456–1462. [CrossRef]
13. Wang, Z.; Gao, K.; Sun, Y.; Zhang, Z.; Zhang, S.; Liang, Y.; Li, X.; Ren, L. Effects of Bionic Units in Different Scales on the Wear Behavior of Bionic Impregnated Diamond Bits. *J. Bionic Eng.* **2016**, *13*, 659–668. [CrossRef]
14. Sidorenko, D.; Mishnaevsky, L., Jr.; Levashov, E.; Loginov, P.; Petrzhik, M. Carbon nanotube reinforced metal binder for diamond cutting tools. *Mater. Design.* **2015**, *83*, 536–544. [CrossRef]
15. Spierings, A.B.; Leinenbach, C.; Kenel, C.; Wegener, K. Processing of metal-diamond composites using selective laser melting. *Rapid. Prototyp. J.* **2015**, *21*, 130–136. [CrossRef]
16. Kabir, M.R.; Richter, H. Modeling of processing-induced pore morphology in an additively-manufactured Ti-6Al-4V alloy. *Materials* **2017**, *10*, 145. [CrossRef] [PubMed]
17. Zhou, Y.; Zeng, X.; Yang, Z.; Wu, H. Effect of crystallographic textures on thermal anisotropy of selective laser melted Cu-2.4Ni-0.7Si alloy. *J. Alloy Compd.* **2018**, *743*, 258–261. [CrossRef]
18. Yang, Y.; Chen, J.; Song, C.; Wang, D.; Bai, Y. Current status and progress on technology of selective laser melting of metal parts. *Laser Optoelectron. Prog.* **2018**, *55*, 011401. [CrossRef]
19. Mirkoohi, E.; Tran, H.-C.; Lo, Y.-L.; Chang, Y.-C.; Lin, H.-Y.; Liang, S.Y. Analytical modeling of residual stress in laser powder bed fusion considering part's boundary condition. *Crystals* **2020**, *10*, 337. [CrossRef]

20. Zhang, X.; Tang, S.; Zhao, H.; Guo, S.; Li, N.; Sun, B.; Chen, B. Research status and key technologies of 3D printing. *J. Mater. Eng.* **2016**, *44*, 122–128.
21. Zhang, C.; Ren, Y.; Chen, X. The development situation of selective laser melting metal powder based on 3D printing. *Appl. Mech. Mater.* **2014**, *518*, 12–18. [CrossRef]
22. Gu, D.; Shen, Y. Research status and technical prospect of rapid manufacturing of metallic part by selective laser melting. *Aeronaut. Manuf. Tech.* **2012**, *404*, 32–37.
23. Sharma, V.; Pandey, P.M. Recent advances in turning with textured cutting tools: A review. *J. Clean. Prod.* **2016**, *137*, 701–735. [CrossRef]
24. Artini, C.; Muolo, M.L.; Passerone, A. Diamond-metal interfaces in cutting tools: A review. *J. Mater. Sci.* **2012**, *47*, 3252–3264. [CrossRef]
25. Zhao, X.; Duan, L. A review of the diamond retention capacity of metal bond matrices. *Metals* **2018**, *8*, 307. [CrossRef]
26. Kruth, J.-P.; Mercelis, P.; Van Vaerenbergh, J.; Froyen, L.; Rombouts, M. Binding mechanisms in selective laser sintering and selective laser melting. *Rapid Prototyp. J.* **2005**, *11*, 26–36. [CrossRef]
27. West, C.; Wang, X. Modeling of selective laser sintering/selective laser melting. In Proceedings of the Laser 3D Manufacturing IV. P SPIE. 2, San Francisco, CA, USA, 8 January–2 February 2017; Volume 10095, p. 1009506. [CrossRef]
28. Reis, L.; Amaral, P.M.; Li, B.; de Freitas, M.; Guerra Rosa, L. Evaluation of the residual stresses due to the sintering process of diamond-metal matrix hot-pressed tools. *Theor. Appl. Fract. Mec.* **2008**, *49*, 226–231. [CrossRef]
29. Liu, F.; Yang, Y.; Pan, B. Influence of tungsten coating on microstructure and thermal damage of brazed diamonds. *Surf. Eng.* **2019**, *35*, 29–36. [CrossRef]
30. Liu, W.; Pan, F.; Yang, H.; Yu, G.; Chen, Z.; Tan, S. Influence of magnetic treatment parameters on mechanical properties of hot-pressing sintering iron-based diamond bit matrix. *Geol. Sci. Technol. Inf.* **2018**, *37*, 269–274. [CrossRef]